ISBN: 978-3-95450-261-5 ISSN: 2673-7000 doi: 10.18429/JACoW-NAPAC2025-THP026

DEVELOPMENT OF SUPERCONDUCTING ADAPTIVE GAP UNDULATOR (SC-AGU)*

T. Tanabe, M. Musardo, D. Hidas, T. Brookbank, J. Rank, P. N'Gotta
Brookhaven National Laboratory, National Synchrotron Light Source-II, Upton, NY, USA

Abstract

The concept of the Adaptive Gap Undulator has been proposed for some time. However, utilizing a permanent magnet-based device complicates the design due to the necessity of independent gap control for each segment and, in the case of an in-vacuum undulator, the requirement for a flexible continuity sheet to mitigate image current heating. The adoption of SC magnets eliminates these concerns. The SC-AGU prototype will comprise three sections of magnetic arrays with a total length of 60 cm, with the central section featuring a smaller gap than the end units. To achieve this, a UHV chamber will be designed for eventual fabrication, incorporating a non-uniform aperture that conforms to the beam envelope. Furthermore, to maintain a constant fundamental photon energy and maximize on-axis spontaneous emission, each SC section will be engineered with distinct period lengths, with the central section possessing a shorter period than the end units.

This paper presents the methodology for end-field analysis, encompassing detailed simulations to characterize the magnetic field distribution at the extremities of each magnetic array. Particular emphasis is placed on the impact of field quality at junctions and its influence on radiation properties, ensuring the optimization of on-axis spontaneous emission while preserving the electron beam's 'stay-clear' area and mitigating impedance constraints imposed by the undulator magnet structure. Other practical information such as power supplies, quench detection and vacuum chamber design is also included.

INTRODUCTION

For storage-ring insertion devices (IDs), an increase in ID length necessitates a commensurately wider gap to satisfy the stay-clear aperture constraint. To mitigate this limitation, the constant-resonant-energy undulator (CREU) was proposed [1]. Although the CREU is conceptually ideal, fabricating an undulator with a continuously varying period length along the axial direction is pragmatically challenging. The adaptive-gap undulator (AGU) simplifies the magnetic architecture relative to the CREU [2], particularly when implemented in a superconducting-undulator (SCU) configuration, as it incorporates no moving components.

Our R&D prototype aims to surpass the performance of conventional NbTi-wire-based devices. Nb_3Sn conductors have been demonstrated to generate superior magnetic fields [3]. However, the standard wind-and-react (W&R) process demands reaction at exceedingly high temperatures and protracted annealing intervals. The National Institute for Materials Science (NIMS) is developing ultra-thin A15 composite wires, 0.03–0.05 mm in diameter, to facilitate highly flexible Rutherford cables [4]. Such cables can follow a react-and-wind (R&W) regimen, thereby simplifying yoke fabrication and obviating high-temperature baking.

The principal issues yet to be resolved are: 1) devising a phasing strategy for each segment that preserves an acceptably low phase error; 2) ensuring that R&W Nb_3Sn conductors are deployed with a minimum bending radius exceeding 20 mm to prevent degradation of current-carrying capacity, thereby necessitating the conception of a yoke geometry capable of accommodating this requirement; and 3) developing a novel vacuum chamber featuring a variable aperture.

MAGNET DESIGN

For R&D purpose, an AGU with three short sections (~20 cm each) is proposed. Table 1 shows the essential parameters of magnetic array in each segment. Segments are tuned to the same resonant energy.

Table 1: AGU Array Parameters

	Segment 1 [Center]	**Segment 2 & 3 [Sides]**
Period Length λ_u, [mm]	14.0	15.5
Deflection Parameter K	2.2	2.05
Pole Gap [mm]	5.0	6/5

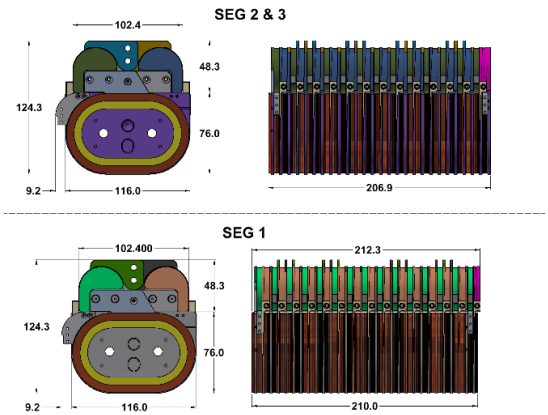

Figure 1: Yoke design for three segments.

The R&W NbSn3 wire requires the minimum bending radius of 20 mm to avoid degradation of performance. Therefore, a novel yoke design with spools for each half period was developed. Figure 1 shows the yoke design for segment 2 and 3 in the upper position, and segment 1

ISBN: 978-3-95450-261-5 ISSN: 2673-7000 doi: 10.18429/JACoW-NAPAC2025-THP026

structure is delineated in the lower position. For each segment, two grooves from both ends have corrector winding underneath of the main winding.

SELECTION OF SC WIRES

0.8 ϕ react-and-wind (R&W) cables fabricated with ultra-thin Nb_3Sn wires, developed by the National Institute for Materials Science (NIMS), will be employed for the primary winding in segment 1, where the maximum current density is demanded. The principal objective of this R&D effort is to determine the optimal phasing between segments. To that end, conventional multifilamentary NbTi wire with a Cu:SC ratio of 0.9:1 and Formvar insulation will be utilized in segments 2 and 3. An additional segment 2 yoke will be wound with second-generation MgB_2 wire developed by Hypertech, Inc. [5] to investigate an alternative solution suitable for 10 K operation. MgB_2 wire is also sensitive to mechanical stress; however, our novel yoke design accommodates this constraint while maintaining satisfactory performance. NbTi wire with a diameter of 0.5 mm will be used for the corrector windings.

PHASING DESIGN

Expected residual field integrals at the interface of adjacent magnetic array units, which arise from differing deflection parameter values between them, will be compensated for by auxiliary windings at the terminus of each magnetic array segment. These windings will be optimized to mitigate the angular deflections experienced by the electron beam at array junctions as it traverses the device and to refine the phasing requirement between units. Such trajectory perturbations can drastically affect the on-axis emission between the segments, resulting in a perturbation of the radiation phase for the entire device. Therefore, a rigorous design study is conducted to define the optimal end-section winding configuration that can improve the electron trajectory straightness and phasing, thereby enhancing the overall magnetic performance of the device.

Each segment end is equipped with two windings, resulting in a total of twelve independent power supplies, each capable of delivering up to 24 A. The main coil power supplies are designed to generate currents up to 1000 A. Because the corrector coils are wound beneath the main coils at the segment extremities, both their spatial positioning and excitation current can be adjusted to optimize inter-segment phasing. Figure 2 presents the magnetic field profile of a slightly shortened version of the device, while the calculated electron trajectory—demonstrating the effect of a minor correction field at the entrance—is illustrated in Fig. 3.

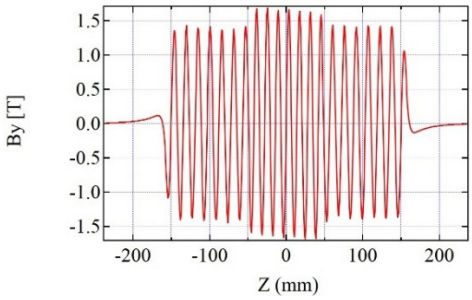

Figure 2: Magnetic flux density profile along the longitudinal axis.

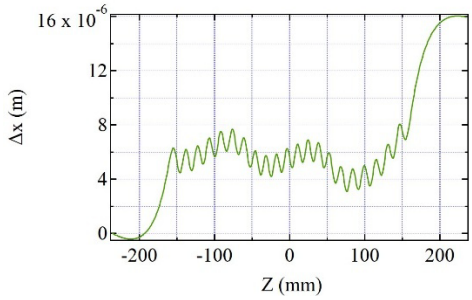

Figure 3: Trajectory with small negative field integral at the entrance.

POWER SUPPLIES AND QUENCH DETECTOR

The two main power supplies for this project are Sorensen (Ametek) 1000 A, 10 V, 10 kW systems. Although these units incorporate their own internal regulation circuitry, they operate in conjunction with an externally developed control loop designed in-house. This control scheme employs high-precision DCCT (fluxgate magnetometer) units manufactured by Danisense within the feedback loop to achieve ultra-stable current regulation. A single controller unit manages the feedback loops for both high-current supplies and also serves as the interface platform with the EPICS machine control system, which is extensively utilized throughout the NSLS-II storage ring. This integration facilitates potential incorporation of the equipment into broader future projects. Each trim power supply for the correction coils comprises two bipolar channels, rated at 24 A and 18 V, with independent control. This configuration provides a total of 12 independent control channels—four per array segment pair within the scope of the project.

The quench detection system is built around the COMPACTRIO (cRIO-9066) platform from National Instruments—an FPGA-based controller operating at 667 MHz, equipped with an 8-slot chassis capable of accommodating a variety of National Instruments C Series measurement modules. The detector employs five NI-9239 modules, each providing four isolated 24-bit ±10 V analog-to-digital conversion channels, with simultaneous sampling capabilities of up to 50,000 samples per second. This configuration enables 20 isolated and independently monitored detection channels for the coil array. The remaining slots in

ISBN: 978-3-95450-261-5 ISSN: 2673-7000 doi: 10.18429/JACoW-NAPAC2025-THP026

the FPGA chassis allow for future expansion to 32 channels, if required.

The FPGA system is housed within a 3RU enclosure that also integrates the necessary power supplies and interface circuitry to transmit trip signals to both the trim and main power supply controllers, as well as the safety interlock system. The quench detector and its associated wire harness interface are mounted within a Varistar control cabinet, positioned above the main and trim power supplies for array segment number two. Additionally, a dedicated resistor array box is mounted adjacent to the test dewar to suppress electrical noise.

METER LONG AGU IN NSLS2U

A design study for the upgrade of the NSLS-II storage ring has commenced, employing a novel lattice architecture based on the "Complex Bend Magnet" concept [6]. The electron beam energy is projected to increase from 3 GeV to 4 GeV, with the bare lattice horizontal emittance targeted at 20 pm·rad and the vertical emittance at 8 pm·rad. Figure 4 presents brightness curves comparing a 5 m-long superconducting adaptive-gap undulator (SC-AGU), two 2 m-long SCU14 devices, and the currently utilized 3 m-long IVU20. The assumed beam current is 400 mA, the relative energy spread is 4.9×10^{-4}, and both the horizontal and vertical beta functions are set at 2 m. The assumed insertion device (ID) design parameters for each segment are as follows:

λ_u=14mm K=2.09 B=1.60 gap=6.5mm
λ_u =13mm K=2.21 B=1.82 gap=5.0mm
λ_u =12mm K=2.33 B=2.08 gap=4.0mm
λ_u =13mm K=2.21 B=1.82 gap=5.0mm
λ_u =14mm K=2.09 B=1.60 gap=6.5mm.

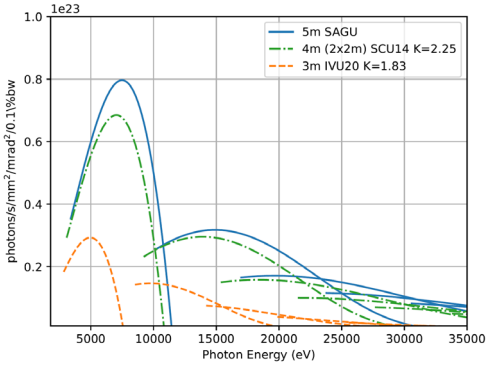

Figure 4: Brightness curves of various IDs in NSLS2U.

VACUUM CHAMBER DESIGN

A novel vacuum chamber has been designed wherein the vacuum aperture conforms to the vertical stay-clear envelope, while the segmented region within the insula ting vacuum preserves the required pole gaps. A small-scale prototype of the AGU vacuum chamber has been developed, featuring a central flat vacuum gap of 3 mm. The inner gaps in the outer sections are gradually expanded to mitigate geometric impedance. A 1 mm-thick stainless steel sheet is affixed to the contoured side pieces. A cross-sectional model is illustrated in Figure 5. Figure 6 presents the total deformation under the opposite condition—ultra-high vacuum (UHV) inside and atmospheric pressure outside.

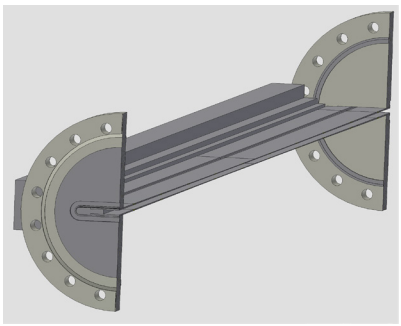

Figure 5: SC-AGU vacuum chamber model.

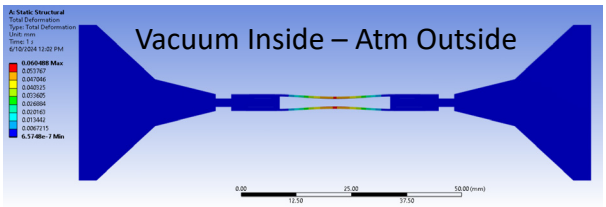

Figure 6: Static structural total deformation of the AGU vacuum chamber. UHV inside and atmosphere outside.

CONCLUSION

The Superconducting Adaptive Gap Undulator (SC-AGU) prototype has been fabricated with support from the U.S. Department of Energy (DOE) through the Laboratory Directed Research and Development (LDRD) Program. The SC-AGU provides a fundamental advantage by eliminating the necessity for excessively long, vertically wound magnets typically required in extended devices. To attain performance exceeding that of conventional NbTi-based systems, the prototype employs wind-and-react Nb_3Sn wire developed by the National Institute for Materials Science (NIMS) in Japan.

REFERENCES

[1] S.C. Gottschalk *et al.*, "Gap-tapered undulators for high-photon-energy synchrotron radiation production," *AIP Conf. Proc. 521*, p. 348, 1999. doi:10.1063/1.1291813

[2] O. V. Chubar *et al.*, "Spectral performance of segmented adaptive-gap in-vacuum undulators for storage rings," in *Proc. IPAC'12*, New Orleans, LA, USA, May 2012, pp. 765-767.

[3] I. Kesgin *et al.*, "Fabrication and testing of 18-mm-period, 0.5-m-long Nb_3Sn superconducting undulator," *IEEE Trans. Appl. Supercond.*, vol. 31, no. 5, pp. 1–5, Aug. 2021. doi:10.1109/tasc.2021.3057846

[4] M. Sugano, A. Kikuchi, H. Kitaguchi, G. Nishijima, and T. Yagai, "Uniaxial tensile stress tolerance of ultra-thin Nb_3Sn composite wires and twisted cables," *IEEE Trans. Appl. Supercond.*, vol. 34, no. 5, pp. 1–5, Aug. 2024. doi:10.1109/tasc.2024.3355355

ISBN: 978-3-95450-261-5 ISSN: 2673-7000 doi: 10.18429/JACoW-NAPAC2025-THP026

[5] F. Wan, M. D. Sumption, M. A. Rindfleisch, C. J. Thong, M. J. Tomsic, and E. W. Collings, "High performance, advanced-internal-magnesium-infiltration (AIMI) MgB_2 wires processed using a vapor-solid reaction route," *Supercond. Sci. Technol.*, vol. 33, no. 9, p. 094004, Jul. 2020. doi:10.1088/1361-6668/ab9ef1

[6] V. V. Smaluk and T. V. Shaftan, "Realizing Low-Emittance Lattice Solutions With Complex Bends," in *Proc. IPAC'19*, Melbourne, Australia, May 2019, pp. 1906-1908. doi:10.18429/JACoW-IPAC2019-TUPRB105